CLIPB4 is a central node in the protease network that regulates humoral immunity in *Anopheles gambiae* mosquitoes

Xiufeng Zhang[a], Shasha Zhang[a,b], Junyao Kuang[c], Kathleen A. Sellens[d], Bianca Morejon[a], Sally A. Saab[e], Miao Li[a], Eve C. Metto[d], Chunju An[b], Christopher T. Culbertson[d], Mike A. Osta[e], Caterina Scoglio[c], Kristin Michel[a]

[a] Division of Biology, Kansas State University, Manhattan, KS, USA
[b] Department of Entomology, College of Plant Protection, China Agricultural University, Beijing, China
[c] Department of Electrical and Computer Engineering, Kansas State University, Manhattan, KS 66506, USA
[d] Department of Chemistry, Kansas State University, Manhattan, KS, USA
[e] Department of Biology, American University of Beirut, Beirut, Lebanon

Author contact information: Xiufeng Zhang, xiufengz@ksu.edu; Shasha Zhang, zhangshasha@bjfc.cc; Junyao Kuang, junyao.kuang@crownbio.com; Kathleen A. Sellens, sellens2@yahoo.com; Bianca Morejon, bmorejon744@ksu.edu; Sally A. Saab, ssaab4@jh.edu; Eve C. Metto, emetto@d.umn.edu; Miao Li, limiao@ksu.edu; Mike A. Osta, mo07@aub.edu.lb; Chunju An, 201118@cau.edu.cn; Christopher T. Culbertson, culbert@ksu.edu; Caterina Scoglio, caterina@ksu.edu; Kristin Michel, kmichel@ksu.edu.

Short Title: CLIPB4's central role in mosquito melanization

Corresponding Author:
Kristin Michel
Division of Biology
Kansas State University
Manhattan, KS 66506, USA
Telephone: +1-785-532-0161
Email: kmichel@ksu.edu

Number of Tables: 1 main and 4 online supplementary tables
Number of Figures: 6 main and 6 online supplementary figures

Word count: 7,788

Key words: *Anopheles gambiae*, clip domain serine protease, insect immunity, melanization, phenoloxidase, serpin

Abstract

Insect humoral immune responses are regulated in part by protease cascades, whose components circulate as zymogens in the hemolymph. In mosquitoes, these cascades consist of clip domain serine proteases (cSPs) and/or their non-catalytic homologs (cSPHs), which form a complex network, whose molecular make-up is not fully understood. Using a systems biology approach, based on a co-expression network of gene family members that function in melanization and co-immunoprecipitation using the serine protease inhibitor (SRPN)2, a key negative regulator of the melanization response in mosquitoes, we identify the cSP CLIPB4 from the African malaria mosquito *Anopheles gambiae* as a central node in this protease network. *CLIPB4* is tightly co-expressed with *SRPN2* and forms protein complexes with SRPN2 in the hemolymph of immune-challenged female mosquitoes. Genetic and biochemical approaches validate our network analysis and show that CLIPB4 is required for melanization and antibacterial immunity, acting as a prophenoloxidase (proPO)-activating protease, which is inhibited by SRPN2. In addition, we provide novel insight into the structural organization of the cSP network in *An. gambiae*, by demonstrating that CLIPB4 is able to activate proCLIPB8, a cSP upstream of the proPO-activating protease CLIPB9. These data provide the first evidence that, in mosquitoes, cSPs provide branching points in immune protease networks and deliver positive reinforcement in proPO activation cascades.

Introduction

The African malaria mosquito, *Anopheles gambiae*, is one of the efficient vectors of life-threatening human malaria parasites. In 2021, approximately 247 million cases and 619,000 deaths were reported of malaria worldwide (1). Despite the availability of an effective, albeit non-sterilizing, vaccine, vector population control remains the most common and effective malaria prevention tool, which is threatened by insecticide resistance in target mosquito populations. Novel vector population control schemes, utilizing gene drive, male sterility, and *Wolbachia*-based methods (2–4) in part rely on detailed molecular understanding of mosquito physiology. For this reason, mosquito innate immunity has received much attention, as it is a major determinant of vector competence and survival of mosquitoes within and across their life stages (5–7).

Protease cascades play a central role in innate immunity, regulating blood clotting and complement activation in mammals, hemolymph clotting in horseshoe crabs, and melanization and Toll signaling pathway activation in insects (8–10). Their activation leads to proteolytic cleavage of a series of inactive protease zymogens between a prodomain and the protease domain, which then cleave downstream key immune factors, ensuring a fast, often within minutes, activation of antimicrobial immunity. In insects, these cascades consist of so-called clip-containing serine proteases (cSPs), a large protein family (consisting of 5 subfamilies, A-E), which is characterized by one or more clip pro-domains and one or more protease domains with trypsin-like specificity, and their homologs (cSPHs), which have lost one or more residues of the catalytic triad required for proteolytic activity. Our knowledge of the molecular makeup of these cascades is mainly derived from insect model species that are either large in size, enabling biochemical investigations of their hemolymph (e.g. *Manduca sexta* (11) and *Tenebrio molitor* (12)), or hold an excellent genetic and molecular tool box (in case of *Drosophila melanogaster* (13,14)).

At their core, canonical insect immune protease cascades consist of a modular serine protease (ModSP), which upon recognition of foreign molecular patterns, self-activates and then cleaves and activates a cSP in the subfamily C that in turn cleaves and activates a terminal cSP in the subfamily B (cSP-B) (15–17). Activation of melanization, an insect specific immune response proceeds through the terminal cSP-B pro-phenoloxidase activating protease (PAP) that cleaves the zymogen pro-phenoloxidase (proPO) to active phenoloxidase, a key enzyme in the conversion of aromatic amino acids to quinones that ultimately polymerize to eumelanin on foreign surfaces. Clip serine protease homologs support the proPO cascade, as they are required for effective

96 activation of PO on foreign surfaces (18–20). To prevent uncontrolled spread and over-activation
97 of responses, serine protease inhibitors in the serpin family tightly control mammalian and
98 arthropod immune protease cascades.

99 In *An. gambiae*, melanization is a readily selectable parasite resistance mechanism that
100 garnered much attention in hopes of exploiting the molecular underpinnings of this resistance
101 mechanism for malaria control purposes (21,22). In addition, the gene families encoding cSPs and
102 cSPHs in *An. gambiae*, known as CLIPs, and proPOs have undergone large expansions, raising
103 the question whether regulation of melanization is more complex than in other insects (23–26). To
104 date, the melanization response in *An. gambiae* has been analyzed genetically using RNAi (27)
105 combined with at least five experimental readouts, often with the implicit or explicit assumption
106 that identified CLIPs contribute biochemically to proPO activation. Thus far, two *An. gambiae*
107 cSPs, CLIPB9 and B10 have been identified as PAPs, based on their ability to revert increased
108 systemic melanization induced genetically by knockdown (kd) of *An. gambiae serpin-2* (*SRPN2*)
109 and to cleave purified *M. sexta* proPO *in vitro* (28,29). These data indicate that, based on the
110 canonical model of proPO activation cascades, melanization in *An. gambiae* depends on at least
111 two such cascades, characterized by CLIPB9 and B10, respectively. Based on genetic and
112 biochemical data, CLIPB8 is located further upstream of CLIPB9 (30). All three CLIPB proteases
113 required for proteolytic activation of proPO are inhibited by serpins (SRPNs). Of the 18 SRPNs
114 annotated in the *An. gambiae* genome, only SRPN2 has been shown to control systemic
115 melanization (7,31). It inhibits effectively both PAPs, CLIPB9 and B10, and also CLIPB8, albeit
116 to a lesser degree (28–30). Several additional CLIPBs, including CLIPB3, 4, 14 and 17 also
117 contribute to melanization; however the molecular function and placement of these additional
118 CLIPBs in proPO activation cascades is unknown (32,33). The only cSP in the CLIPC family to
119 contribute to melanization is CLIPC9, presumably through the action of cleavage of either PAP,
120 which however remains to be demonstrated (34).

121 In addition to cSPs, melanization in *An. gambiae* is regulated positively by a core module of
122 cSPHs, consisting, in hierarchical order, of SPCLIP1, CLIPA8 and CLIPA28. This module is
123 located genetically upstream of CLIPC9 and downstream of the thioester-containing protein TEP1
124 (6,32,34–36). Melanization is also regulated negatively by cSPHs, including CLIPA2 and A14
125 (32,37). While the precise mechanism(s) by which *An. gambiae* cSPHs regulate melanization
126 (positively or negatively) are unknown, observations in *An. gambiae* suggest that cSPHs contribute

127 to the opsonization of microbial surfaces by TEP1 and the leucine-rich repeat proteins LRIM1 and
128 APLC1 (35,38), and, based on data from other insect species, to PO activity by mediating proPO
129 cleavage by PAPs (19,39,40). In addition, melanization of rodent and human malaria parasites in
130 *An. gambiae* is inhibited by two c-type lectins, CTL4 and CTLMA2 (41,42), which presumably
131 bind to sugar moieties on the parasite surface and prevent melanization locally. The rodent malaria
132 parasite melanization phenotype induced by *CTL4* kd has been used successfully to identify some
133 of the cSPs and cSPHs mentioned above (e.g. (32)).
134 However, despite the significant number of studies summarized above, our understanding of
135 cSP cascades that control melanization in *An. gambiae* remains incomplete, and more than 80% of
136 the 110 annotated CLIPs await experimental exploration. To guide the experimental analysis of
137 *An. gambiae* cSPs and to identify putative key regulators of the melanization response, we describe
138 here a novel systems biology approach to study melanization in insects, combining transcriptomic
139 network and proteomic analyses. Using this approach, we identify the cSP CLIPB4 as a central
140 node in the protease network that regulates melanization in *An. gambiae* and characterize its
141 placement in the proPO activation cascade using a combination of genetic and biochemical
142 approaches.
143

144 **Materials and Methods**

145 *Mosquito cultures*

146 The *An. gambiae* G3 strain was obtained from the Malaria Research and Reference Reagent
147 Resource Center (MR4) at CDC and reared as described previously (29). For egg production,
148 females were provided a blood meal of commercial heparinized horse blood (Plasvacc USA) using
149 parafilm as a membrane stretched across glass feeders connected to a 37°C circulating water bath.

150 Anopheles gambiae *Melanization Gene Co-expression Network (AgMelGCN)*

151 The AgMelGCN was constructed according to (43). Genes of interest (GOIs), represented as nodes
152 were selected based on published evidence either confirming experimentally their role in
153 melanization or confirming phylogenetically their membership in protein families known to
154 contribute to melanization in mosquitoes. The GOI list contained 191 genes, including 9
155 prophenoloxidases (PPO), 14 thioester-containing proteins (TEP), 23 C-type lectins (CTL), 16
156 leucine-rich repeat immune proteins (LRIM), 18 serpins (SRPN), 4 putative modular serine

157 proteases (ModSP), 20 clip domain serine protease A family proteins (CLIPA), 29 CLIPB, 12
158 CLIPC, 13 CLIPD, 32 CLIPE, and SP24D, a putative ModSP. Their raw expression values were
159 collated from 257 unique physiological conditions assessed in 30 separate transcriptome studies,
160 and z-score conversion was performed for normalization under each condition. Two genes were
161 considered co-expressed and connected by edges if the Pearson Correlation coefficient (PCC) of
162 their expression vectors was above the 3% fitted sliding threshold. PCCs were rescaled based on
163 the reversed curve of the fitted sliding thresholds to assign edge weights. The network was
164 visualized using Gephi 0.9.2 (44) using the Fruchterman-Reingold force-directed algorithm (45).
165 Network communities were assigned with the Girvan-Newman algorithm (46). Four measures
166 were applied for node centrality, evaluating the edge abundance connected to a single node: node
167 strength (sum of connected edge weights), eigenvector centrality, betweenness centrality and
168 harmonic closeness centrality (47). In addition, s-core decomposition analysis was performed. In
169 the case of a weighted network, the s-core subgraph consists of all nodes i with node strengths $s(i) >$
170 s, where s is a threshold value. We define the threshold value of the s_n-core as $s_{(n-1)} = \min s(i)$,
171 among all nodes i belonging to the $s_{(n-1)}$-core network. The s_n-core is found by the iterative removal
172 of all nodes with strengths $s(i) \leq s_{(n-1)}$ (48).

173 *SRPN2 Co-immunoprecipitation (Co-IP) and Mass Spectrometric Analysis*

174 Female mosquitoes were challenged by microinjection of 69 nl lyophilized *Micrococcus luteus* in
175 water (OD_{600} =0.55, Sigma-Adrich) per mosquito, and hemolymph was collected from 420 female
176 mosquitoes into 1x Roche Protease Inhibitor in PBS by proboscis clipping 19 h post infection. The
177 SRPN2 antiserum, produced previously (29), was affinity purified using the pH 7.2 coupling buffer
178 with AminoLink™ Plus Immobilization kit (ThermoFisher Scientific), and stored in PBS. Co-IP
179 was performed with Pierce™ Protein A Magnetic Beads (ThermoFisher Scientific), and beads
180 were rinsed with the buffer PBSOg (PBS with 0.7% w/v n-Octyl-BD- Glucopyranoside). Mosquito
181 hemolymph was equally split for two co-IP reactions: one with 40 µl 1:1 slurry of PBSOg-
182 containing magnetic beads cross-linked with 30 µg of purified SRPN2 antibody; and the other with
183 40 µl 1:1 slurry of PBSOg-containing control magnetic beads. Hemolymph was incubated with
184 the beads for 1.5 h at room temperature with constant rotation. The unbound fractions were
185 removed and magnetic beads were washed twice with PBSOg followed by four washes with
186 UltraPure™ water (Invitrogen). Bound proteins were eluted into 20 µl 0.1% TFA (w/v,
187 trifluoroacetic acid in water) in each co-IP. Samples were shipped to the Nevada Proteomics Center

188 (University of Nevada, Reno) for identification via LC-Orbitrap-MS. Contaminants were removed
189 with 2-D Clean-up kit (GE Healthcare), and in-tube trypsin digestion was performed. Resultant
190 peptides were run through a Michrom Paradigm Microdialysis Liquid Chromatography and
191 Michrom CaptiveSpray coupled to a Thermo LTQ Orbitrap XL with Electron-transfer dissociation
192 (ETD). MS spectra were analyzed using Sequest (IseNode in Proteome Discoverer version
193 2.2.0.388, Thermo Fisher Scientific). Sequest searches of ANOGA_uniprot_20210804.fasta
194 (25565 entries) were performed with the following settings: digestion enzyme trypsin, maximal
195 missed cleavage = 2, fragment ion mass tolerance = 0.60 Da, and a parent ion tolerance = 50 PPM.
196 Carbamidomethyl of cysteine was specified as a fixed modification, while oxidation of methionine,
197 acetylation of the N-terminus and phosphorylation of serine were specified as variable
198 modifications. Scaffold (version 5.1.0, Proteome Software Inc.) was used to validate peptide and
199 protein identifications. Peptide probability was calculated by the Peptide Prophet algorithm (49)
200 with Scaffold delta-mass correction, and a ≥95.0% identification cut-off. Protein probabilities were
201 assigned by the Protein Prophet algorithm (50). Proteins that contained similar peptides and could
202 not be differentiated based on MS analysis alone were grouped to satisfy the principles of
203 parsimony. In the SRPN2 Co-IP sample, a protein was considered present if protein probability
204 was greater than 99.0%, and 2 minimal unique peptides were identified in the sequence. A protein
205 was removed from the SRPN2 Co-IP list if at least one minimal peptide was detected in the control
206 sample. Proteome Discoverer SequestHT scores were listed at the protein level to rank the final
207 identification list.

208 *Expression and purification of recombinant proteins proCLIPB4 and proCLIPB4$_{Xa}$*

209 To produce recombinant proCLIPB4, its full coding region, including the signal peptide, was
210 amplified by PCR using gene specific primers (Table S1) and *An. gambiae* adult cDNA as template.
211 The forward primer contained a NotI site at 5'-end, and the reverse primer included three glycine
212 codons, six histidine codons, a stop codon, and a HindIII site at the 3'-end. The PCR product was
213 digested by NotI and HindIII, and inserted into the same restriction sites in the transfer vector
214 pFastBac1 (Invitrogen). The resulting proCLIPB4-6His-pFastBac1 plasmid was used as a template
215 to produce the mutant proCLIPB4$_{Xa}$-6His-pFastBac1.To utilize commercial Factor Xa (New
216 England Biolabs), the predicted activation site LTDR^{107} of proCLIPB4 was replaced with IEGR^{107}.
217 Site-directed mutagenesis was introduced to proCLIPB4-6His-pFastBac1 by Vent DNA
218 polymerase (New England Biolabs) with mutagenic primers (Table S1), DpnI (New England

219 Biolabs) digestion and NEB10β transformation. The resulting proCLIPB4$_{Xa}$-6His-pFastBac1 was
220 confirmed by Sanger Sequencing. The DNA segments containing proCLIPB4-6His and
221 proCLIPB4$_{Xa}$-6His, respectively, were transferred from pFastBac1 to pOET3 (Oxford Expression
222 Technologies) by BamHI and HindIII sites, creating proCLIPB4-6His-pOET3 and proCLIPB4$_{Xa}$-
223 6His-pOET3, respectively. The pFastBac1 and pOET3 transfer vectors were used to produce
224 corresponding CLIPB4 baculoviruses using the Sf9 cell line by means of Bac-to-Bac system
225 (Invitrogen) or flashBAC-Baculovirus Expression system (Genway Biotech). Large-scale
226 expression was performed using Sf9 suspension cultures at 2×10^6 cells/mL cell density in Sf-900
227 II serum-free medium (Invitrogen). Baculoviruses were inoculated at multiplicity of infection
228 (MOI) of 1, and expression media were harvested 48 h post infection. Recombinant proteins were
229 purified as described previously (28–30). In brief, cells were cleared by centrifugation, and
230 expression medium was dialyzed and subjected to column chromatography with Ni-NTA agarose
231 (Qiagen) and Q Sepharose Fast Flow (Cytiva). Eluted fractions were screened by immunoblot with
232 THE™ His Tag Antibody. Combined fractions were concentrated with buffer exchange (20 mM
233 Tris, 50 mM NaCl, pH 8.0) in Amicon™ Ultra-10K centrifugal units. Recombinant proteins were
234 stored at -80°C until future use. Recombinant proCLIPB8$_{Xa}$, proCLIPB8, proCLIPB9$_{Xa}$,
235 proCLIPB9 and SRPN2 were expressed and purified as described previously (29,30).

236 *SDS-PAGE and Immunoblot*

237 Protein samples were mixed with SDS sample buffer containing β-mercaptoethanol, and denatured
238 at 95°C for 5 min. Proteins were separated on SDS-PAGE gels (Bio-Rad) with constant voltage at
239 120V followed by 180V. SDS-PAGE gels were stained with EZ-Run Protein Gel Staining Solution
240 (Fisher) and de-stained with Milli-Q water. For immunoblot, proteins were transferred onto
241 nitrocellulose membranes (GE Healthcare) at 10V constant voltage using Owl™ Semidry
242 Electroblotting Systems (ThermoFisher Scientific). Membranes were incubated with 5% dry milk
243 in 1xTBST (0.05% Tween-20) at room temperature (RT) for 1 h, followed by primary antibody
244 incubation diluted in 0.5% dry milk in 1xTBST (4°C overnight or RT for 2 h). Blots were washed
245 three times with 1xTBST for 20 min each at RT. Membranes were further incubated with diluted
246 secondary antibodies in 0.5% dry milk 1xTBST at RT for 1 h. Protein signals were developed by
247 Alkaline Phosphate (AP) Conjugate Substrate Kit (Bio-Rad) and Amersham™ ECL™ Western
248 Blotting Detection Reagents (GE Healthcare) for AP-conjugated and HRP-conjugated secondary

249 antibodies, respectively. Images were captured by CCD camera of Azure Biosystems 300 for ECL
250 development.

251 *Factor Xa activation of IEGR-mutated recombinant proteins*

252 Factor Xa activation of recombinant proCLIPB4$_{Xa}$ is described in the legend of online suppl. Fig.
253 S3. Activation of proCLIPB8$_{Xa}$ and proCLIPB9$_{Xa}$ was performed as described previously (29,30).

254 *SRPN2 inhibition of CLIPB4*

255 To produce active CLIPB4, 630 ng of recombinant proCLIPB4$_{Xa}$ was incubated with 1 µg of
256 Factor Xa in a total volume of 11 µl with Factor Xa activation buffer at 37°C overnight. Two
257 negative controls were set up in parallel, where proCLIPB4$_{Xa}$ or Factor Xa was replaced with the
258 same volume of Factor Xa activation buffer. Activated CLIPB4$_{Xa}$ (154 ng/per reaction) was mixed
259 with recombinant (r)SRPN2 at molar ratios of 1:1 or 1:10 (proCLIPB4$_{Xa}$:SRPN2). After incubation
260 at room temperature for 15 min, the reaction mixtures were subjected to immunoblot analysis with
261 mouse anti-His, rabbit anti-SRPN2 or rabbit anti-CLIPB4 as primary antibodies. For Mass
262 spectrometry identification, reactions were set up as described as above, and subjected to SDS-
263 PAGE. After Coomassie brilliant blue staining, the band of interest (~72 kDa) was excised. In-gel
264 trypsin digestion and Electrospray ionization mass spectrometry (ESI-MS, Bruker Daltonics HCT
265 Ultra) were performed at the Biotechnology/Proteomics Core Facility (Kansas State University).
266 MS results were analyzed in Scaffold 4.0. To determine the stoichiometry of inhibition, 90 ng of
267 Factor Xa-activated rCLIPB4$_{Xa}$ was mixed with rSRPN2 at molar ratios of 0:1, 0.5:1, 1:1, 2:1, 4:1,
268 and 6:1 (rSRPN2:rCLIPB4$_{Xa}$) in reaction buffer 20 mM Tris, 150 mM NaCl, pH 8.0 supplemented
269 with 3 µg BSA. Reactions were incubated at room temperature for 15 min. The residual amidase
270 activity was determined with IEARpNA substrate at OD_{405} as described above. IEARase activity
271 of Factor Xa was measured in parallel and subtracted from the above reactions of
272 rSRPN2:rCLIPB4$_{Xa}$. Amidase activity at molar ratio of 0:1 (rSRPN2:rCLIPB4$_{Xa}$) was defined as
273 100%. All assays were performed in triplicate.

274 *Purification of PPO1&2 from M. sexta larval hemolymph*

275 Prophenoloxidase 1&2 (*Ms*PPO1&2) was purified from *M. sexta* hemolymph similarly to
276 published methodology (51). Briefly, hemolymph was collected into 100% ammonium sulfate (AS)
277 at 0℃ from 5th instar Day 2 *M. sexta* larvae. Fraction of 38-48% AS precipitation was dissolved in
278 buffer A (10 mM KPi, pH 6.8, 500 mM NaCl, 0.5 mM reduced L-Glutathione), and dialyzed
279 against buffer A. Bio-Gel HT Hydroxyapatite column (Bio-Rad) was utilized to separate proteins

280 via a linear gradient of 10-100 mM KPi in buffer A. Two microliters per fraction was assayed with
281 200 µl 2 mM Dopamine hydrochloride in 50 mM NaPi, pH 6.5 with and without 0.1%
282 cetylpyridinium chloride (CPC, w/v) in 96-well plates, and absorbance change was monitored at
283 470 nm in EPOCH 2 microplate reader (BioTek). Fractions containing CPC-activated PO activity
284 were combined, and concentrations of $MgCl_2$ and $CaCl_2$ were adjusted to 1 mM each. The protein
285 solution was applied twice through a Concanavalin A Sepharose 4B column (GE Healthcare),
286 equilibrated in 20 mM Tris, pH 7.4, 0.5 M NaCl, 1 mM $MgCl_2$, 1 mM $CaCl_2$. Column flow-through
287 fraction was adjusted to 1 M AS, and loaded onto a Phenyl Sepharose 6 Fast Flow low sub column
288 (Cytiva), equilibrated in 0.1 M KPi, pH 7.1, 1 M AS. Elution was performed with a descending
289 linear gradient of 0.1 M KPi, pH 7.1, 1 M AS to 0.01 M KPi, pH 7.1. Fractions with CPC-activated
290 PO activity were pooled and concentrated to 1.1 ml using Amicon™ Ultra-15 30K centrifugal
291 units (Merck Millipore). Proteins were separated by Sephacryl S-300 column (Cytiva),
292 equilibrated in 10 mM MOPS, pH 7.2, 0.5 M NaCl. Fractions containing CPC-activated PO
293 activity were pooled and concentrated to 4.6 mg/ml by Amicon™ Ultra-15 30K units. Equal
294 volume of glycerol was mixed with purified *Ms*PPO1&2, and the purified zymogen was stored at
295 -80°C at 2.3 mg/ml in 5 mM MOPS, pH 7.2, 0.25 M NaCl, 50% glycerol.

296 *ProPO activation by CLIPB4$_{Xa}$ using M. sexta plasma and purified MsPPO1&2*

297 To evaluate the contribution of CLIPB4 on proPO activity, *M. sexta* plasma and purified
298 *Ms*PPO1&2 were utilized as described previously (29). Naïve hemolymph was collected from a
299 cut proleg of 5th instar Day 3 *M. sexta* larvae, and centrifuged at 5,000 g, 4°C for 5 min to remove
300 hemocytes and cell debris. Factor Xa was used to activate proCLIPB4$_{Xa}$ as described in online
301 suppl. Fig. S3. For PO enzymatic activity plate assay, in each well, 1 µl plasma was mixed with 3
302 µl Factor Xa-proCLIPB4$_{Xa}$ activation mixture per well, supplemented to 10 µl with buffer B (20
303 mM Tris, 20 mM NaCl, 6.7 mM $CaCl_2$, pH 7.5). Three negative controls were set up, replacing
304 Factor Xa, proCLIPB4$_{Xa}$, and both with buffer B, respectively for a final reaction volume of 10 µl.
305 Three technical replicates were set up per reaction, and incubated at RT for 15 min. Per well, 200
306 µl 2 mM Dopamine hydrochloride was added in the buffer 50 mM NaPi, pH 6.5. Absorbance was
307 monitored at 470 nm at RT for 1 h. For PO activity assay with purified MsPPO1&2, per well, 1
308 µg purified *Ms*PPO1&2 (4 µl at 250 ng/µl) was mixed with 5 µl of activation mixture and 3 µl of
309 buffer B for a total reaction volume of 12 µl. One additional negative control was included by
310 mixing 1 µg purified *Ms*PPO1&2 with 8 µl buffer B. Three technical replicates were set up for

311 each reaction and incubated at RT for 1 h. Dopamine hydrochloride was added as described above
312 and absorbance was monitored at 470 nm at RT for 1 h. One unit of PO activity was defined as
313 ΔA470/min = 0.001.

314 *ProPO cleavage by CLIPB4$_{Xa}$ using M. sexta plasma and purified MsPPO1&2*

315 To detect cleavage of *Ms*PPO1&2, we performed immunoblots with rabbit anti-*Ms*PPO1&2
316 primary antibody (51). Naïve *M. sexta* plasma was first diluted to 1:20 in 20 mM Tris, 150 mM
317 NaCl, pH 8.0. Reactions were set up by mixing 1 µl diluted plasma, 3 µl Factor Xa activation
318 buffer or 3 µl each from Factor Xa proCLIPB4$_{Xa}$ RT activation mixtures (including negative
319 controls), and 6 µl buffer B for a 10 µl total reaction volume. Three additional samples were
320 prepared by mixing 3 µl each from Factor Xa proCLIPB4$_{Xa}$ RT activation mixtures and 7 µl buffer
321 B. Reactions were incubated at RT for 20 min. For purified *Ms*PPO1&2, reactions were set up by
322 mixing 2 µl purified *Ms*PPO1&2 (250 ng/µl, 500 ng) with 6 µl Factor Xa activation buffer or 6 µl
323 each from Factor Xa proCLIPB4$_{Xa}$ activation mixtures (see online suppl. Fig. 3). Reactions were
324 incubated at RT for 20 min. For immunoblot, 1.2 µl of each reaction (containing 75 ng of
325 *Ms*PPO1&2) was mixed with 8.8 µl water, and boiled at 95°C for 5 min with SDS sample buffer.
326 Samples were separated on 7.5% SDS-PAGE gels, and probed with *Ms*PPO1&2 antibody. In
327 addition, CLIPB9$_{Xa}$-*Ms*PPO1&2 reactions were included as a positive control. Briefly, to obtain
328 activated CLIPB9$_{Xa}$, 2.5 µg of purified recombinant proCLIPB9$_{Xa}$ was mixed with 1 µg Factor Xa,
329 and Factor Xa activation buffer in a total reaction volume of 25 µl, and incubated at 37°C overnight.
330 Two negative control reactions were set up and incubated in parallel, in which recombinant
331 proCLIPB9$_{Xa}$ and Factor Xa were replaced with the same volume of Factor Xa activation buffer,
332 respectively.

333 *CLIPB4 activation of proCLIPB8 and proCLIPB9*

334 To test whether CLIPB4 cleaves recombinant proCLIPB8 and/or proCLIPB9, proCLIPB4$_{Xa}$ was
335 activated by Factor Xa at 37°C. 154 ng of Factor Xa-activated CLIPB4$_{Xa}$ was incubated with 100
336 ng proCLIPB8 or 100 ng proCLIPB9 at RT for 15 min. Recombinant proCLIPB8$_{Xa}$ or
337 proCLIPB9$_{Xa}$ was activated by Factor Xa similarly as described previously (29,30), and 100 ng of
338 activated CLIPB8$_{Xa}$ or CLIPB9$_{Xa}$ was used as a positive control. Samples were subjected to SDS-
339 PAGE and immunoblot using mouse anti-His, rabbit anti-CLIPB8, or rabbit anti-CLIPB9
340 antibodies. To measure the enzymatic activity of cleaved CLIPB8, 610 ng of recombinant
341 proCLIPB4$_{Xa}$ (102 ng/µl) was incubated at 37 °C for 10 h with 1 µg (1 µg/µl) Factor Xa,

342 supplemented to 21 µl with Factor Xa activation buffer. 72 ng of activated $CLIPB4_{Xa}$ was
343 incubated with 450 ng proCLIPB8 (225 ng/µl) at room temperature for 1 h. Reactions were
344 supplemented with 200 µl of 100 µM N-benzoyl-Phe-Val-Arg-p-nitroanilide (FVR-pNA, EMD
345 Chemicals) in 0.1 M Tris-HCl, pH 8.0, 0.1 M NaCl, 5 mM $CaCl_2$ and amidase activity was
346 measured continuously at OD_{405} for 30 min. 450 ng of activated $CLIPB8_{Xa}$ was used as a positive
347 control. One unit of CLIPB8 activity was defined as ΔA405/min = 0.001. All activity assays were
348 performed in triplicate.

349 *Double-stranded RNA (dsRNA) synthesis and RNAi experiments*

350 DsRNA synthesis and adult female mosquito injections were performed as described previously
351 (29). Primers are listed in Table S1 for T7-tagged gene-specific amplification of *CLIPB4*. Primers
352 were adapted from previous studies for dsRNA synthesis of *SRPN2*, *GFP*, *CLIPB8*, and *LacZ*
353 (29,30,52). In single gene knockdown (kd) experiments, 3 to 4-day old adult female mosquitoes
354 were injected each with 207 ng of dsRNA in a total volume of 69 nl. For kd control, mosquitoes
355 were injected with the same quantity of the non-related dsRNA of either *Green Fluorescent*
356 *Protein* (ds*GFP*) or *β-galactosidase* (ds*LacZ*). For double knockdowns (dkd), mosquitoes were
357 injected with 138 nL of a 1:1 dsRNA mixture containing 1.5 µg/µl of each dsRNA. For dkd
358 controls, ds*GFP* was added to compensate the total dsRNA dose to 414 ng/mosquito.

359 *Melanization phenotype analysis*

360 To assess CLIPB4's impact on melanization, two assays were utilized, Melanization-associated
361 Spot Assay (MelASA) and SRPN2 depletion-induced melanotic pseudotumor formation. To
362 quantify melanotic excreta, MelASA was performed in the standard format (50
363 mosquitoes/experimental cup) as described previously (34), with or without bacterial challenge.
364 For MelASAs after bacterial challenge, dsRNA-injected mosquitoes were allowed to recover for
365 60 h and injected each with 50.6 nl of 1x PBS, OD_{600}=1.5 *Escherichia coli* (resuspended in 1x
366 PBS, same below), OD_{600}=1.5 *Staphylococcus aureus*, and OD_{600}= 0.4 *M. luteus* (*Micrococcus*
367 *lysodeikticus* lyophilized cells ATCC, No. 4698, Sigma - Aldrich), respectively. Clean P8-grade
368 white filter papers (Fisher) were inserted into the bottom of the experimental cups after bacterial
369 challenge and removed 12 h later. For MelASAs without bacterial challenge, clean filter papers
370 were inserted immediately after dsRNA injection, and removed 60 h later. All MelASAs were
371 performed with five independent biological replicates using different mosquito generations.
372 Collected filters papers were imaged under white epi-illumination without filters in an Alpha

373 Imager System, and analyzed by Fiji is Just Image J (FIJI, Version 2.1.0) (53) using custom FIJI
374 macros. To quantify melanotic pseudotumor formation, mosquitoes were dissected when mortality
375 reached 70% in the ds*SRPN2*/ds*GFP* group. Abdominal walls were prepared as described
376 previously (7) and examined under 40× magnification with Axio Imager A1 microscope (Zeiss)
377 equipped with AxioCam MR5 (Zeiss). Image processing, and abdomen melanized area calculation
378 were performed in ImageJ software as described previously (29,54). Five independent biological
379 replicates were performed using 20 mosquitoes per treatment. All statistical analyses were
380 performed using GraphPad Prism (ver. 9.5.1, GraphPad Software).
381

382 **Results**

383 *Co-expression analysis of putative melanization genes identifies CLIPB4 as a central node*

384 In the absence of a genome-wide protein-protein interaction network for *An. gambiae*, we used
385 gene co-expression as a proxy to identify proteins that are likely to inhabit the same space at the
386 same time. To facilitate the identification of possible protein-protein interactions, and specifically
387 SRPN2-cSP interactions controlling melanization, we therefore constructed an undirected gene
388 co-expression network of all *An. gambiae* genes belonging to gene families experimentally shown
389 to contribute to melanization, which we named the *Anopheles gambiae* Melanization Gene Co-
390 expression Network (AgMelGCN) (Fig. 1a). In total, the AgMelGCN contains 178 nodes (genes)
391 and 1229 edges (co-expression links between gene pairs) (online suppl. Tables S2 and S3). To
392 reveal the central nodes of AgMelGCN, we performed an *s*-core analysis (s=11.14). The core
393 contained 25 genes, of which nine play a role in melanization (APL1C, CLIPA2, A8, B4, B10,
394 CLIPC9, CTL4, CTLMA2, LRIM1; online suppl. Table S2). To identify key cSPs in the network,
395 we calculated two centrality measures, node strength (weight sum of all node's edges) and
396 harmonic closeness centrality (sum of shortest paths to all other nodes within the full network)
397 (47). Of all annotated cSPs, CLIPB4 was the highest ranked node in either centrality measure
398 (online suppl. Table S2, Fig. 1b). In AgMelGCN, CLIPB4 was connected by a weighted edge to
399 44 other nodes, including seven SRPNs; notably, the SRPN2-CLIPB4 edge had the highest weight
400 among all SRPN nodes connected to CLIPB4 (Fig. 1b; online suppl. Table S3). SRPN2 was
401 connected to 18 nodes, including five cSPs, all in the CLIPB sub-family (Fig.1c; online suppl.
402 Table S3), of which the SRPN2-CLIPB4 edge possessed the highest weight. Overall, these results

403 suggested that CLIPB4 is a central node in the AgMelGCN whose expression most closely
404 resembled that of SRPN2.

405 *SRPN2 and CLIPB4 interact in adult mosquito hemolymph*

406 Since SRPN2 is a critical factor affecting the melanization process, we aimed to identify its closely
407 associated proteins in the hemolymph of adult mosquitoes. Using co-immunoprecipitation, we
408 identified 21 proteins bound directly or indirectly to SRPN2 in the hemolymph of adult female
409 mosquitoes 24 h post challenge with lyophilized *M. luteus* bacteria (Table 1). Among these, six
410 genes were co-expressed with SRPN2 in AgMelGCN, including TEP15, CLIPB4, CLIPA14,
411 SRPN11, CLIPA9 and CLIPA6 (Fig. 1c, Table 1 and online suppl. Table S3). Among annotated
412 cSPs and cSPHs, CLIPB4 was ranked the highest in SRPN2 Co-IP MS protein scores, warranting
413 further examination of the interaction between SRPN2 and CLIPB4.

414 *CLIPB4 is a serine protease with trypsin-like specificity*

415 To investigate its biochemical function(s), we expressed recombinant *An. gambiae* proCLIPB4
416 zymogen *in vitro*. The determinants of enzyme specificity were predicted to be D^{305}, G^{332} and G^{343}
417 (online suppl. Fig. S1a), suggesting that CLIPB4 is a trypsin-like protease that cleaves its substrate
418 after arginine or lysine residues (55). As the endogenous activating enzyme of CLIPB4 is unknown,
419 a mutant (proCLIPB4$_{Xa}$) was produced by replacing its putative activation site ^{104}LTDR^{107} (56)
420 with ^{104}IEGR^{107} (online suppl. Fig. S1b), enabling recognition and cleavage by commercially
421 available bovine Factor Xa. We produced and purified recombinant proCLIPB4$_{Xa}$ zymogen
422 (rproCLIPB4$_{Xa}$) tagged with 6His at its C-terminus (Fig. S2a). Coomassie stain, His antibody and
423 anti-CLIPB4 antibody detected rproCLIPB4$_{Xa}$ (37.9 kDa) at the expected molecular weight.
424 Recombinant proCLIPB4$_{Xa}$ was cleaved by Factor Xa after incubation at 37°C and RT, generating
425 a fragment corresponding to the expected size of the CLIPB4 catalytic domain (rCLIPB4$_{Xa}$, Fig.
426 S3a and c). Recombinant CLIPB4$_{Xa}$ exhibited amidase activity, using IEAR*p*NA substrate, while
427 rproCLIPB4$_{Xa}$ did not (Fig. S3b and S3d). As noted in previous works, Factor Xa also utilized
428 IEAR*p*NA as a substrate (28–30). These results together support that, consistent with our construct
429 design, Factor Xa is able to cleave and activate rCLIPB4$_{Xa}$-6His.

430 *SRPN2 irreversibly inhibits CLIPB4* in vitro

431 Based on the AgMelGCN and co-IP results, we hypothesized that SRPN2 is a direct inhibitor of
432 CLIPB4. To test this hypothesis, we determined (i) if SRPN2 and CLIPB4 form inhibitory protein
433 complexes and (ii) if SRPN2 decreases CLIPB4 amidase activity in a concentration-dependent

434 manner. Purified rSRPN2, tagged N-terminally with 6-His tag, was incubated with rCLIPB4$_{Xa}$ at
435 room temperature for 15 min at two different molar ratios, 1:1 or 10:1 (rSRPN2: rCLIPB4$_{Xa}$). In
436 SDS-PAGE and immunoblot analyses of these reactions a higher molecular weight band appeared
437 at 72 kDa, which was detected with anti-His, anti-SRPN2 and anti-CLIPB4 antibodies (Fig. 2A,
438 2B and 2C). ESI-MS analysis on the 72 kDa band (online suppl. Table S4) detected 15 and 2
439 peptides for SRPN2 and CLIPB4, respectively, corresponding to 11 and 2 unique peptides for each,
440 confirming that SRPN2 and CLIPB4 form a SDS-stable protein complex. CLIPB4$_{Xa}$ amidase
441 activity against IEAR*p*NA decreased with increasing amount of rSRPN2, with a stoichiometry of
442 inhibition (SI) of 1.4 (Fig. 2d), demonstrating that SRPN2 functions as an efficient inhibitor of
443 CLIPB4.

444 CLIPB4kd *is required for the phenotypes induced by SRPN2 depletion*

445 Previously, *SRPN2*kd was shown to reduce the longevity of female mosquitoes and to induce
446 melanotic pseudotumor formation (7). Our biochemical data support that SRPN2 directly inhibits
447 the activity of CLIPB4, and we hypothesized that CLIPB4 is required for the phenotypes induced
448 by SRPN2 depletion. To test this hypothesis, we performed genetic epistasis experiments, inducing
449 gene knockdown by long dsRNA injection. Adult female *An. gambiae* were injected with dsRNAs
450 targeting *CLIPB4*, *SRPN2*, and both *CLIPB4* and *SRPN2*, respectively. Injection of *dsGFP* was
451 used as a control. *CLIPB4* knockdown was significant and specific as determined by immunoblot
452 (online suppl. Fig. S4). Injection of ds*SRPN2* did not affect CLIPB4 protein levels.

453 We first evaluated the effect of *CLIPB4*kd on survival comparing the survival curves between
454 the four different treatment groups, and we also monitored the survival of uninjected mosquitoes.
455 *SRPN2*kd significantly shortened longevity as compared to the uninjected controls and ds*GFP*-
456 control treatment (Fig. 3a and b). In contrast, *CLIPB4*kd had no effect on lifespan as compared to
457 the controls. Importantly, ds*CLIPB4/SRPN2*-treatment substantially and significantly increased
458 mosquito longevity as compared to *SRPN2*kd mosquitoes, returning longevity to those of
459 uninjected and ds*GFP*-control treated mosquitoes.

460 We then evaluated the effect of *CLIPB4*kd on melanization, using the appearance of melanotic
461 tumors as a read-out (Fig. 3c). Injection of ds*GFP* or ds*CLIPB4* alone did not cause melanization
462 (data not shown). In contrast, *CLIPB4*kd in a *SRPN2*-depleted background, significantly affected
463 the *SRPN2*kd melanization phenotype, reducing the average total melanotic area for each dissected
464 mosquito abdomen by 54 %, however, not completely reverting the SRPN2 depletion phenotype.

465 We also used the recently established melanization-associated spot assay (MelASA) to evaluate
466 the contribution of CLIPB4 on the SRPN2 depletion phenotype (34). The standard format (50
467 mosquitoes/cup) was adopted and melanotic excreta were recorded for the four treatment groups.
468 *CLIPB4*kd alone exhibited similar melanotic excreta area compared to that of the negative control,
469 ds*GFP*. SRPN2 depletion, however, significantly increased melanotic excreta of female
470 mosquitoes. Double knockdown of *SRPN2* and *CLIPB4* significantly reduced the excreta
471 compared to *SRPN2* single knockdown, but did not completely abolish the SRPN2 depletion
472 phenotype (Fig. 3d). Taken together, the silencing experiments strongly suggest that *CLIPB4* is
473 epistatic to *SRPN2* and therefore downstream of this serpin in the proPO activation cascade.

474 *CLIPB4 is required for melanization after microbial challenge*

475 Since CLIPB4 is required for melanization induced by SRPN2 depletion, we hypothesized that
476 CLIPB4 is broadly required for melanization in antimicrobial immunity. To test the hypothesis,
477 we first conducted MelASAs after challenge with bacteria (*S. aureus*, *M. luteus*, and *E. coli*)
478 (online suppl. Fig. S5). Without bacterial challenge, only small amounts of melanotic excreta were
479 observed in the ds*GFP*-injected and *CLIPB4*kd treatment groups, consistent with our previous
480 observation in Fig. 3d. Each bacterial challenge increased significantly melanotic excreta in the
481 ds*GFP*-injected group as compared to ds*GFP*-injected mosquitoes treated with PBS, supporting
482 that bacterial treatment indeed induces the melanization immune response. The induction of
483 melanotic excreta by bacterial challenge was dampened in the *CLIPB4*kd treatment groups.
484 Independent of bacterial species, melanotic excreta were reduced by about 50% in *CLIPB4*kd
485 mosquitoes as compared to ds*GFP*-injected mosquitoes, demonstrating that melanization in
486 response to bacterial infection is broadly dependent on CLIPB4.

487 *CLIPB4 functions as a proPO activating enzyme*

488 The shortage of hemolymph collectable from *An. gambiae* mosquitoes can be overcome by using
489 the *M. sexta* model system as a source of proPO, as *M. sexta* PPO1&2 share the conserved cleavage
490 site with eight of the nine proPOs encoded in the *An. gambiae* genome (7). Activated $CLIPB4_{Xa}$
491 was incubated with *M. sexta* plasma, followed by immunoblot analysis using anti-*M. sexta* proPO
492 antibody. A doublet band around 80 kDa in *M. sexta* plasma represents heterodimeric proPO
493 consisting of 79-kDa proPO1 and 80-kDa proPO2 (51). Addition of activated $CLIPB4_{Xa}$ to *M.*
494 *sexta* plasma resulted in the appearance of a 70-kDa doublet band corresponding to *M. sexta* active
495 PO (Fig. 4a). The same doublet band was observed in the plasma supplemented with activated

496 CLIPB9$_{Xa}$, which we identified previously as a functional PAP in *An. gambiae* (29). PO activity
497 of plasma increased in the presence of active CLIPB4$_{Xa}$ (Fig. 4c). These results confirm that the
498 proteolytic activity of CLIPB4 promotes proPO cleavage and PO activity. To determine the
499 placement of CLIPB4 in the proPO activation cascade in *An. gambiae*, we next tested whether
500 CLIPB4 can directly cleave and activate proPO. ProPO1&2 was purified from 5th instar *M. sexta*
501 larvae (Fig. S2c). By Coomassie Blue staining and immunoblot analysis with MsPPO antibody, a
502 dimer was observed around 80 kDa, consistent with previous observations of purified full length
503 *M. sexta* proPO1 and 2 (51). We then incubated Factor Xa-activated rCLIPB4$_{Xa}$ with purified *M.*
504 *sexta* proPO, using again rCLIPB9$_{Xa}$ as a positive control. Neither rproCLIPB9$_{Xa}$ zymogen nor
505 Factor Xa alone were able to cleave MsPPO1&2, while active rCLIPB9$_{Xa}$ cleaved purified
506 MsPPO1&2 to produce the PO1&2 band at 70 kDa (Fig. 4b). Similarly, neither rproCLIPB4$_{Xa}$
507 zymogen nor Factor Xa alone cleaved PPO1&2, but active rCLIPB4$_{Xa}$ cleaved proPO1&2 (Fig.
508 4b), leading to an increase in PO activity (Fig. 4d), demonstrating that CLIPB4 functions as a PAP.
509 <u>*CLIPB4 cleaves and activates CLIPB8*</u>
510 We next explored whether CLIPB4 also promotes PO activity indirectly by activating the PAP
511 zymogen proCLIPB9 (29) and/or proCLIPB8, a protease upstream of CLIPB9 in the melanization
512 cascade in *An. gambiae* (30). To test whether CLIPB4 can cleave proCLIPB8 and/or B9 *in vitro*,
513 active CLIPB4$_{Xa}$ was incubated with wild-type recombinant proCLIPB8 and proCLIPB9,
514 respectively, followed by immunoblot analysis using either anti-His antibody or anti-CLIPB8 and
515 anti-CLIPB9 antibodies, respectively. In the reaction of active CLIPB4$_{Xa}$ with proCLIPB8
516 zymogen, anti-His and anti-CLIPB8 antibodies detected a 36 kDa band, corresponding to the
517 CLIPB8 protease domain, which was also detected in the control reaction of proCLIPB8$_{Xa}$
518 incubated with Factor Xa (Fig. 5a and b). In contrast, addition of active CLIPB4$_{Xa}$ (or Factor Xa)
519 did not result in the cleavage of proCLIPB9 (Fig. 5c and d), suggesting that CLIPB4 is not directly
520 upstream of CLIPB9. To evaluate whether cleavage of recombinant proCLIPB8 by CLIPB4$_{Xa}$
521 results in CLIPB8 activation, we measured the amidase activity of the reaction mixtures using
522 FVR as a substrate (30). Each of the five control reactions, containing proCLIPB8, proCLIPB8$_{Xa}$,
523 Factor Xa, proCLIPB4$_{Xa}$, and proCLIPB4$_{Xa}$/proCLIPB8, respectively did not exhibit amidase
524 activity. Active CLIPB4$_{Xa}$ showed limited amidase activity, which was increased threefold when
525 active CLIPB4$_{Xa}$ was incubated with proCLIPB8 prior to the addition of substrate (Fig. 5e).

526 Together with the immunoblot results (Fig. 5a and 5b), FVRase activity assay supports that
527 CLIPB4 specifically cleaves and activates CLIPB8.
528 To examine this phenomenon *in vivo*, ds*LacZ*, ds*CLIPB4* and ds*CLIPB8* were injected in adult
529 female mosquitoes that were challenged by *S. aureus* post the dsRNA injection recovery.
530 Hemolymph was collected 10 h after challenge and subjected to SDS-PAGE and immunoblot
531 detection (Fig. 6). The Apolipophorin-II (APOII) was utilized as a loading control. CLIPB8 was
532 depleted with ds*CLIPB8* treatment, serving as a positive control for CLIPB8 antibody detection.
533 Ten hours after bacterial challenge, a clear reduction of CLIPB8 was observed in ds*LacZ* compared
534 to the naïve control in two independent experiments, suggesting that CLIPB8 in the hemolymph
535 was rapidly utilized in the acute immune response (57). The CLIPB8 reduction, mediated by *S.*
536 *aureus* challenge, was rescued with ds*CLIPB4* treatment in two independent experiments,
537 providing additional support that CLIPB4 acts upstream of CLIPB8 in the hierarchical cSP cascade
538 regulating melanization in *An. gambiae*.
539

540 **Discussion**

541 Mosquitoes interact with a broad range of organisms across the symbiosis continuum and deploy
542 melanization as a broad-spectrum immune defense against many organisms they encounter (58).
543 The melanization of microbial surfaces in *An. gambiae* requires opsonization through TEP1 and
544 the activity of PO to produce eumelanin, which depends on the action of cascades made up of cSPs
545 and cSPHs. This study identifies CLIPB4 as an important factor required for melanization in
546 response to microbial infection. CLIPB4 was previously shown to contribute to melanization of
547 glass beads and malaria parasites in *CTL4* kd mosquitoes (32,33). Here we show that CLIPB4 is
548 also required for melanotic tumor formation exerted by the depletion of SRPN2 in adult female
549 mosquitoes, demonstrating that its contribution to melanization is not limited to specific surfaces,
550 and suggesting that CLIPB4 is fundamental to eumelanin production. Indeed, our data demonstrate
551 that CLIPB4 functions as a PAP, mediating proPO activation *ex vivo* and *in vitro*. In addition to
552 CLIPB9 and B10, CLIPB4 is the third PAP identified in *An. gambiae* (28,29). In all three cases,
553 their ability to cleave and activate proPO *in vitro*, was demonstrated using purified proPO1 and 2
554 from the hemolymph of *M. sexta*. Given that *An. gambiae* PPO5 and 6, the most abundant proPOs
555 in the hemolymph of adult female *An. gambiae*, share the same activation cleavage site with *M.*
556 *sexta* proPO1&2, it is highly likely that all three CLIPBs are bona fide PAPs in *An. gambiae* (7,59).

557 The existence of three PAPs, each constituting a terminal protease in a cSP cascade, suggests
558 that melanization in adult female *An. gambiae* is regulated by at least three proPO activation
559 cleavage cascades. Similarly, *M. sexta* proPO activation is regulated by at least two proPO
560 activation cascades, utilizing either PAP3 or PAP1/PAP2 as the terminal proteases to cleave proPO
561 (60,61). Likewise, two distinct proPO activation cascades regulate melanization in the
562 lepidopteran species, *Helicoverpa amigera* (15,62). In *An. gambiae*, possibly not all three PAPs
563 contribute equally to activate proPO. Expression of CLIPB4 in adult female *An. gambiae*, as
564 measured by RNA-Seq is much higher than that of CLIPB9, B10, and any other CLIPB whose kd
565 causes a melanization phenotype (Buchon and Michel, unpublished), suggesting that CLIPB4
566 protein, based on its abundance, contributes more to proPO activation than other PAPs. This
567 observation may also explain why neither CLIPB8, B9 nor B10 were identified in the SRPN2 co-
568 IP analyses, despite previous data demonstrating that CLIPB9 and SRPN2 form inhibitory
569 complexes in *An. gambiae* hemolymph (29). Whether, in addition to protein concentration, the
570 activation of the three *An. gambiae* PAPs depends on the type of microbial challenge, as observed
571 in *H. amigera* (62), is currently under investigation.
572 In addition to its PAP function, CLIPB4's central role in melanization in female *An. gambiae*
573 is further manifested by its ability to cleave and activate proCLIPB8. This function was
574 demonstrated *in vitro* by biochemical studies and *in vivo*, as *CLIPB4* kd reverts the consumption
575 of CLIPB8 in the hemolymph of adult female *An. gambiae* upon microbial infection. This is of not
576 only the first observation of multiple substrates for a single *An. gambiae* CLIP protease, but also
577 the first demonstration of a CLIPB protease activating another proCLIPB zymogen in mosquitoes,
578 breaking the mold of the classical hierarchy of CLIPC-CLIPB in insect immune protease cascades
579 (63). The observation of CLIPB4 cleavage of CLIPB8 is paralleled in *M. sexta*, where PAP3
580 cleaves proHP5, a cSP-B family member (64). This cleavage of HP5, provides positive
581 reinforcement of proPO activation, as HP5 in turn cleaves HP6, a cSP in the C family, upstream
582 of PAP-1, linking the two proPO activation cascades in *M. sexta* (64). Based on these similar
583 patterns in two evolutionarily distant insect species, it is tempting to speculate that positive
584 reinforcement of proPO activation by cSP-B mediated activation of other cSP-Bs is a common
585 theme in the melanization immune response.
586 Given that the regulation of melanization through proPO activation requires cSPs and cSPHs
587 circulating in mosquito hemolymph prior to immune challenge, we posited that identification of

588 important members in the cSP and cSPH cascades could be identified based on their co-expression.
589 Indeed, the topology of the AgMelGCN, the co-expression network of members of gene families
590 known to contribute to melanization clustered genes with known immune phenotypes into a single
591 community. Using network science approaches, we then identified highly-connected nodes,
592 referred to as hubs, which are integral to scale-free network stability (65). In gene co-expression
593 networks, hub genes and are often relevant for network functionality, either as regulators or
594 because they encode proteins with essential functions (66,67). The nodes with highest connectivity
595 in the AgMelGCN encoded two cSPHs (CLIPA9 and 8), APLC1, and CLIPB4. All four genes
596 encode proteins with known functions in innate immunity. *CLIPA9* kd in *An. gambiae* reduces *P.*
597 *falciparum* oocysts, a phenotype that seems dependent on the presence of an unperturbed
598 microbiota through an unknown mechanism (68). CLIPA8 is a key positive regulator of
599 melanization and part of the cSPH cascade upstream of CLIPC9 (34,36). CLIPA8 is required for
600 melanization of malaria parasites after *CTL4* kd, filamentous fungi, and bacteria (32,69,70). The
601 leucine-rich repeat protein APLC1 contributes to antimicrobial immunity in mosquitoes by
602 stabilizing TEP1 in the hemolymph, preventing its premature activation, and facilitating its
603 delivery to microbial surfaces for opsonization (38,71,72). Likewise, CLIPB4 plays an important
604 role in melanization through its integral roles in the cSP cascade that activates proPO described in
605 this current study. Combined, these data support that gene co-expression networks can indeed be
606 used to identify genes with important functions in mosquito innate immunity, and provide a
607 blueprint for analyses of innate immunity in other insect species and likely other complex
608 physiologies in mosquitoes.

609 The topology of the AgMelGCN also demonstrates the integration of the cSPH and cSP
610 cascades through co-expression of members of each cascade. Our co-IP data indicate that these
611 cascades also at least partially form protein complexes in the hemolymph of *An. gambiae*. We
612 recently showed that CLIPB4 also cleaves CLIPA8 *in vitro*, which is required for CLIPA8 function
613 (57), suggesting that the activation of cSPHs required for melanization is mediated by cSPs and
614 potentially integrated with proPO activation through the formation of higher molecular weight
615 protein complexes. Indeed, higher molecular weight complexes between cSPs and cSPHs and
616 proPO have been described in other insect species, including *M. sexta* (73) and *Bombyx mori* (74),
617 indicating that the formation of such immune complexes is likely an evolutionarily conserved
618 process that is used to optimize proPO activity to microbial surfaces.

619 Based on our results presented herein and published data, we propose the following model of
620 proPO activation in the melanization response of *An. gambiae* (Fig. S6). In adult female
621 mosquitoes, circulating proPO zymogen is activated through the proteolytic activity of three
622 CLIPB proteases, CLIPB4, B9 and B10 (28,29). CLIPB4 also activates proCLIPB8, which
623 activates indirectly proCLIPB9 (30), providing positive reinforcement of proPO activation. Each
624 of these CLIPBs provides an intervention point, as their activity is inhibited directly by SRPN2,
625 reinforcing its role as the main negative regulator of melanization and survival in *An. gambiae*
626 (7,31). This observation is paralleled in *M. sexta*, where serpin-3, the ortholog of SRPN2 inhibits
627 all three identified PAPs (75,76). CLIPC9, currently the only known CLIPC protease required for
628 melanization, is located likely upstream of one or more of the three PAPs and responsible for their
629 proteolytic activation. In turn, based on the canonical proPO activation cascades in other insects,
630 we hypothesize that proCLIPC9 is activated proteolytically through the action of an unknown
631 ModSP. Additionally, melanization of microbial surfaces is further regulated through the activity
632 of a cSPH cascade upstream of CLIPC9 (34,36). Whether, cSPHs also support melanization
633 downstream of PAPs, as observed in other insect species (20,40,62) is currently under
634 investigation. However, despite the existing complexity of this immune protease network, the
635 presence of 110 CLIP genes in the *An. gambiae* genome suggests that additional CLIPB and
636 CLIPC proteases may be involved (23,25,56). We are currently performing a reverse genetic
637 screen to identify the contribution of all annotated *An. gambiae* cSPs and cSPHs to melanization
638 and antimicrobial activity, leveraging the AgMelGCN and recently established *in vivo* bioassays
639 and (34,77). Completion of this screen will describe the entire molecular make-up of the *An.*
640 *gambiae* immune protease network and enable us to identify the molecular interactions within that
641 are critical for vector competence and survival in this important vector species.
642

643 **Acknowledgements**

644 We would like to thank all members of the Michel laboratory for mosquito rearing. We thank the
645 former Michel laboratory members, Ms. Erin Peel for help with the reverse genetic experiments,
646 and Dr. Xin Zhang for initial plasmid construction and expression of recombinant proteins. We
647 are grateful to Dr. John Tomich and the members of the Biotechnology/Proteomics Core Facility,
648 Kansas State University for the MS analysis of the SRPN2/CLIPB4 complexes. We thank Dr.
649 Susan Paskewitz, University of Wisconsin for the kind gift of the CLIPB4 antibody. We

gratefully acknowledge Ms. Rebekah J. Woolsey and Dr. David R. Quilici at the Mick Hitchcock, Ph.D. Nevada Proteomics Center Nevada Proteomics Center, University of Nevada, Reno, for providing the MS analysis of the co-IP experiments. Finally, sincere thanks got to Dr. Michael R. Kanost, Kansas State University, for his continued support and mentorship.

Statement of Ethics

Not applicable to the enclosed manuscript.

Conflict of Interest Statement

Authors disclosed all potential conflict of interest, and none existed for the presented work.

Funding Sources

This work was supported by National Institutes of Health R01AI095842 and R01AI140760, and the USDA National Institute of Food and Agriculture Hatch project 1021223 (all to KM). S.Z. was supported by a scholarship from the China Scholarship Council. This is contribution No. 22-296-J from the Kansas Agricultural Experiment Station. The contents of this article are solely the responsibility of the authors and do not necessarily represent the official views of the funding agencies.

Author Contributions

K.M. conceived the study and C.A., C.T.C., M.A.O., C.S. and K.M. designed the experiments and supervised their execution. X.Z., S.Z., J.K., K.A.S., B.M. V., S.A.S., M.L., E.C.M., and K.M. performed the experiments and analyzed the data. X.Z., S.Z., and K.M. prepared the manuscript, and X.Z., S.Z., M.A.O., C.S., and K.M. revised the manuscript. All authors approved the submitted version.

Data Availability

677 All generated or analyzed data are included within this article and its supplementary material files.

678 Further enquiries should be directed to the corresponding author.

679

680 **References**

681 1. World malaria report 2022 [Internet]. [cited 2023 Jan 16]. Available from:
682 https://www.who.int/teams/global-malaria-programme/reports/world-malaria-report-2022

683 2. Nolan T. Control of malaria-transmitting mosquitoes using gene drives. Philos Trans R Soc
684 Lond B Biol Sci. 2021 Feb 15;376(1818):20190803.

685 3. Ickowicz A, Foster SD, Hosack GR, Hayes KR. Predicting the spread and persistence of
686 genetically modified dominant sterile male mosquitoes. Parasit Vectors. 2021 Sep
687 16;14(1):480.

688 4. Sicard M, Bonneau M, Weill M. Wolbachia prevalence, diversity, and ability to induce
689 cytoplasmic incompatibility in mosquitoes. Curr Opin Insect Sci. 2019 Aug;34:12–20.

690 5. Huff CGG. Studies on the infectivity of plasmodia of birds for mosquitoes, with special
691 reference to the problem of immunity in the mosquito. The American Journal of Hygiene.
692 1927;7(6):706–34.

693 6. Blandin S, Shiao SH, Moita LF, Janse CJ, Waters AP, Kafatos FC, et al. Complement-Like
694 Protein TEP1 Is a Determinant of Vectorial Capacity in the Malaria Vector Anopheles gambiae.
695 Cell. 2004 Mar 5;116(5):661–70.

696 7. Michel K, Budd A, Pinto S, Gibson TJ, Kafatos FC. Anopheles gambiae SRPN2 facilitates
697 midgut invasion by the malaria parasite Plasmodium berghei. EMBO Rep. 2005 Sep;6(9):891–
698 7.

699 8. Pryzdial ELG, Leatherdale A, Conway EM. Coagulation and complement: Key innate defense
700 participants in a seamless web. Front Immunol. 2022;13:918775.

701 9. Cerenius L, Kawabata S ichiro, Lee BL, Nonaka M, Söderhäll K. Proteolytic cascades and
702 their involvement in invertebrate immunity. Trends in Biochemical Sciences.
703 2010;35(10):575–83.

704 10. Kawabata S ichiro, Muta T. Sadaaki Iwanaga: Discovery of the lipopolysaccharide- and beta-
705 1,3-D-glucan-mediated proteolytic cascade and unique proteins in invertebrate immunity. J
706 Biochem. 2010 May;147(5):611–8.

707 11. Kanost MR, Jiang H, Yu XQ. Innate immune responses of a lepidopteran insect, Manduca
708 sexta. Immunol Rev. 2004;198:97–105.

709 12. Park JW, Kim CH, Rui J, Park KH, Ryu KH, Chai JH, et al. Beetle immunity. Adv Exp Med
710 Biol. 2010/01/01 ed. 2010;708:163–80.

711 13. Buchon N, Silverman N, Cherry S. Immunity in Drosophila melanogaster - from microbial
712 recognition to whole-organism physiology. Nature Reviews Immunology. 2014;14(12):796–
713 810.

714 14. Lemaitre B, Hoffmann J. The host defense of Drosophila melanogaster. Annu Rev Immunol.
715 2007/01/05 ed. 2007 Jan;25:697–743.

716 15. Wang Q, Yin M, Yuan C, Liu X, Hu Z, Zou Z, et al. Identification of a Conserved
717 Prophenoloxidase Activation Pathway in Cotton Bollworm Helicoverpa armigera. Front
718 Immunol. 2020;11:785.

719 16. Kanost MR, Jiang H. Clip-domain serine proteases as immune factors in insect hemolymph.
720 Current Opinion in Insect Science. 2015 Oct 1;11:47–55.

721 17. Buchon N, Poidevin M, Kwon HM, Guillou A, Sottas V, Lee BL, et al. A single modular
722 serine protease integrates signals from pattern-recognition receptors upstream of the
723 Drosophila Toll pathway. Proceedings of the National Academy of Sciences of the United
724 States of America. 2009 Jul 28;106(30):12442–7.

725 18. Kwon TH, Kim MS, Choi HW, Joo CH, Cho MY, Lee BL. A masquerade-like serine
726 proteinase homologue is necessary for phenoloxidase activity in the coleopteran insect,
727 Holotrichia diomphalia larvae. Eur J Biochem. 2000;267(20):6188–96.

728 19. Yu XQ, Jiang H, Wang Y, Kanost MR. Nonproteolytic serine proteinase homologs are
729 involved in prophenoloxidase activation in the tobacco hornworm, Manduca sexta. Insect
730 Biochem Mol Biol. 2003;33(2):197–208.

731 20. Jin Q, Wang Y, Hartson SD, Jiang H. Cleavage activation and functional comparison of
732 Manduca sexta serine protease homologs SPH1a, SPH1b, SPH4, and SPH101 in conjunction
733 with SPH2. Insect Biochem Mol Biol. 2022 May;144:103762.

734 21. Collins FH, Sakai RK, Vernick KD, Paskewitz S, Seeley DC, Miller LH, et al. Genetic
735 selection of a Plasmodium-refractory strain of the malaria vector Anopheles gambiae. Science.
736 1986 Oct 31;234(4776):607–10.

737 22. Hurd H, Taylor PJ, Adams D, Underhill A, Eggleston P. Evaluating the costs of mosquito
738 resistance to malaria parasites. Evolution; international journal of organic evolution. 2005
739 Dec;59(12):2560–72.

740 23. Christophides GK, Zdobnov E, Barillas-Mury C, Birney E, Blandin S, Blass C, et al.
741 Immunity-related genes and gene families in Anopheles gambiae. Science. 2002/10/05 ed.
742 2002;298(5591):159–65.

743 24. Neafsey DE, Waterhouse RM, Abai MR, Aganezov SS, Alekseyev MA, Allen JE, et al. Highly
744 evolvable malaria vectors: The genomes of 16 Anopheles mosquitoes. Science. 2015 Jan
745 2;347(6217):1258522–1258522.

746 25. Waterhouse RM, Kriventseva EV, Meister S, Xi ZY, Alvarez KS, Bartholomay LC, et al.
747 Evolutionary dynamics of immune-related genes and pathways in disease-vector mosquitoes.
748 Science. 2007/06/26 ed. 2007;316(5832):1738–43.

749 26. Bartholomay LC, Waterhouse RM, Mayhew GF, Campbell CL, Michel K, Zou Z, et al.
750 Pathogenomics of Culex quinquefasciatus and Meta-Analysis of Infection Responses to
751 Diverse Pathogens. Science. 2010/10/12 ed. 2010;330(6000):88–90.

752 27. Blandin SA, Levashina EA. Reverse genetics analysis of antiparasitic responses in the malaria
753 vector, Anopheles gambiae. Methods Mol Biol. 2008/03/29 ed. 2008;415:365–77.

754 28. Zhang X, Li M, El Moussawi L, Saab S, Zhang S, Osta MA, et al. CLIPB10 is a Terminal
755 Protease in the Regulatory Network That Controls Melanization in the African Malaria
756 Mosquito Anopheles gambiae. Front Cell Infect Microbiol. 2020;10:585986.

757 29. An C, Budd A, Kanost MR, Michel K. Characterization of a regulatory unit that controls
758 melanization and affects longevity of mosquitoes. Cell Mol Life Sci. 2011 Jun;68(11):1929–
759 39.

760 30. Zhang X, An C, Sprigg K, Michel K. CLIPB8 is part of the prophenoloxidase activation system
761 in Anopheles gambiae mosquitoes. Insect Biochem Mol Biol. 2016 Apr;71:106–15.

762 31. Michel K, Suwanchaichinda C, Morlais I, Lambrechts L, Cohuet A, Awono-Ambene PH, et
763 al. Increased melanizing activity in Anopheles gambiae does not affect development of
764 Plasmodium falciparum. Proc Natl Acad Sci U S A. 2006/10/27 ed. 2006;103(45):16858–63.

765 32. Volz J, Müller HM, Zdanowicz A, Kafatos FC, Osta MA. A genetic module regulates the
766 melanization response of Anopheles to Plasmodium. Cellular Microbiology. 2006;8(9):1392–
767 405.

768 33. Paskewitz SM, Andreev O, Shi L. Gene silencing of serine proteases affects melanization of
769 Sephadex beads in Anopheles gambiae. Insect Biochemistry and Molecular Biology.
770 2006;36(9):701–11.

771 34. Sousa GL, Bishnoi R, Baxter RHG, Povelones M. The CLIP-domain serine protease CLIPC9
772 regulates melanization downstream of SPCLIP1, CLIPA8, and CLIPA28 in the malaria vector
773 Anopheles gambiae. PLOS Pathogens. 2020 Oct 12;16(10):e1008985.

774 35. Povelones M, Bhagavatula L, Yassine H, Tan LA, Upton LM, Osta MA, et al. The CLIP-
775 domain serine protease homolog SPCLIP1 regulates complement recruitment to microbial
776 surfaces in the malaria mosquito Anopheles gambiae. PLoS Pathog. 2013;9(9):e1003623.

777 36. Moussawi LE, Nakhleh J, Kamareddine L, Osta MA. The mosquito melanization response
778 requires hierarchical activation of non-catalytic clip domain serine protease homologs. PLOS
779 Pathogens. 2019 Nov 25;15(11):e1008194.

780 37. Nakhleh J, Christophides GK, Osta MA. The serine protease homolog CLIPA14 modulates
781 the intensity of the immune response in the mosquito Anopheles gambiae. The Journal of
782 biological chemistry. 2017 Nov 3;292(44):18217–26.

783 38. Povelones M, Upton LM, Sala KA, Christophides GK. Structure-Function Analysis of the
784 Anopheles gambiae LRIM1/APL1C Complex and its Interaction with Complement C3-Like
785 Protein TEP1. PLOS Pathogens. 2011 Apr 14;7(4):e1002023.

786 39. Kim MS, Baek MJ, Lee MH, Park JW, Lee SY, Soderhall K, et al. A new easter-type serine
787 protease cleaves a masquerade-like protein during prophenoloxidase activation in Holotrichia
788 diomphalia larvae. J Biol Chem. 2002;277(42):39999–40004.

789 40. Ji Y, Lu T, Zou Z, Wang Y. Aedes aegypti CLIPB9 activates prophenoloxidase-3 in the
790 presence of CLIPA14 after fungal infection. Front Immunol. 2022;13:927322.

791 41. Simões ML, Dong Y, Mlambo G, Dimopoulos G. C-type lectin 4 regulates broad-spectrum
792 melanization-based refractoriness to malaria parasites. PLoS Biol. 2022 Jan;20(1):e3001515.

793 42. Osta MA, Christophides GK, Kafatos FC. Effects of mosquito genes on Plasmodium
794 development. Science. 2004 Mar 26;303(5666):2030–2.

795 43. Kuang J, Buchon N, Michel K, Scoglio C. A global gene co-expression network constructed
796 from hundreds of experimental conditions with missing values. BMC Bioinformatics. 2022
797 May 9;23(1):170.

798 44. Bastian M, Heymann S, Jacomy M. Gephi : An Open Source Software for Exploring and
799 Manipulating Networks. :2.

800 45. Fruchterman TMJ, Reingold EM. Graph drawing by force-directed placement. Software:
801 Practice and Experience. 1991;21(11):1129–64.

802 46. Girvan M, Newman MEJ. Community structure in social and biological networks. Proceedings
803 of the National Academy of Sciences. 2002 Jun 11;99(12):7821–6.

804 47. Rodrigues FA. Network centrality: an introduction. arXiv:190107901 [physics] [Internet].
805 2019 Jan 22 [cited 2022 Mar 11]; Available from: http://arxiv.org/abs/1901.07901

806 48. Eidsaa M, Almaas E. s-core network decomposition: A generalization of k-core analysis
807 to weighted networks. Phys Rev E. 2013 Dec 30;88(6):062819.

808 49. Keller A, Nesvizhskii AI, Kolker E, Aebersold R. Empirical statistical model to estimate the
809 accuracy of peptide identifications made by MS/MS and database search. Anal Chem. 2002
810 Oct 15;74(20):5383–92.

811 50. Nesvizhskii AI, Keller A, Kolker E, Aebersold R. A statistical model for identifying proteins
812 by tandem mass spectrometry. Anal Chem. 2003 Sep 1;75(17):4646–58.

813 51. Jiang H, Wang Y, Ma C, Kanost MR. Subunit Composition of Pro-phenol Oxidase from
814 Manduca sexta: Molecular Cloning of Subunit ProPO-p1. Insect Biochemistry and Molecular
815 Biology. 1997 Oct 1;27(10):835–50.

816 52. Kamareddine L, Nakhleh J, Osta MA. Functional Interaction between Apolipophorins and
817 Complement Regulate the Mosquito Immune Response to Systemic Infections. JIN.
818 2016;8(3):314–26.

819 53. Schindelin J, Arganda-Carreras I, Frise E, Kaynig V, Longair M, Pietzsch T, et al. Fiji: an
820 open-source platform for biological-image analysis. Nat Methods. 2012 Jul;9(7):676–82.

821 54. Schneider CA, Rasband WS, Eliceiri KW. NIH Image to ImageJ: 25 years of image analysis.
822 Nat Methods. 2012 Jul;9(7):671–5.

823 55. Perona JJ, Craik CS. Structural basis of substrate specificity in the serine proteases. Protein
824 Sci. 1995 Mar;4(3):337–60.

825 56. Cao X, Gulati M, Jiang H. Serine protease-related proteins in the malaria mosquito, Anopheles
826 gambiae. Insect Biochemistry and Molecular Biology. 2017 Sep 1;88:48–62.

827 57. Saab SA, Zhang X, Morejon B, Michel K, Osta MA. Insight into the structural hierarchy of
828 the protease cascade that regulates the mosquito melanization response. bioRxiv. 2023 Jan
829 1;2023.07.13.548954.

830 58. Bartholomay LC, Michel K. Mosquito Immunobiology: The Intersection of Vector Health and
831 Vector Competence. Annu Rev Entomol. 2018;63:145–67.

832 59. Muller HM, Dimopoulos G, Blass C, Kafatos FC. A hemocyte-like cell line established from
833 the malaria vector Anopheles gambiae expresses six prophenoloxidase genes. J Biol Chem.
834 1999;274(17):11727–35.

835 60. Jiang H, Wang Y, Yu XQ, Zhu Y, Kanost M. Prophenoloxidase-activating proteinase-3 (PAP-
836 3) from Manduca sexta hemolymph: a clip-domain serine proteinase regulated by serpin-1J
837 and serine proteinase homologs. Insect Biochemistry and Molecular Biology. 2003 Oct
838 1;33(10):1049–60.

839 61. Jiang H, Wang Y, Kanost MR. Pro-phenol oxidase activating proteinase from an insect,
840 Manduca sexta: a bacteria-inducible protein similar to Drosophila easter. Proc Natl Acad Sci
841 U S A. 1998;95(21):12220–5.

842 62. Wang Q, Yin M, Yuan C, Liu X, Jiang H, Wang M, et al. The Micrococcus luteus infection
843 activates a novel melanization pathway of cSP10, cSP4, and cSP8 in Helicoverpa armigera.
844 Insect Biochemistry and Molecular Biology. 2022 Aug 1;147:103775.

845 63. Kanost MR, Jiang H. Clip-domain serine proteases as immune factors in insect hemolymph.
846 Curr Opin Insect Sci. 2015 Oct 1;11:47–55.

847 64. Wang Y, Yang F, Cao X, Zou Z, Lu Z, Kanost MR, et al. Hemolymph protease-5 links the
848 melanization and Toll immune pathways in the tobacco hornworm, Manduca sexta. Proc Natl
849 Acad Sci U S A. 2020 Sep 22;117(38):23581–7.

850 65. Barabási AL. Network science. Philosophical Transactions of the Royal Society A:
851 Mathematical, Physical and Engineering Sciences. 2013 Mar 28;371(1987):20120375.

852 66. Hahn MW, Kern AD. Comparative Genomics of Centrality and Essentiality in Three
853 Eukaryotic Protein-Interaction Networks. Molecular Biology and Evolution. 2005 Apr
854 1;22(4):803–6.

855 67. Pierson E, Consortium the Gte, Koller D, Battle A, Mostafavi S. Sharing and Specificity of
856 Co-expression Networks across 35 Human Tissues. PLOS Computational Biology. 2015 May
857 13;11(5):e1004220.

858 68. Dong Y, Manfredini F, Dimopoulos G. Implication of the Mosquito Midgut Microbiota in the
859 Defense against Malaria Parasites. PLOS Pathogens. 2009 May 8;5(5):e1000423.

860 69. Schnitger a. KD, Kafatos FC, Osta M a. The melanization reaction is not required for
861 survival of Anopheles gambiae mosquitoes after bacterial infections. J Biol Chem.
862 2007;282:21884–8.

863 70. Yassine H, Kamareddine L, Osta MA. The mosquito melanization response is implicated in
864 defense against the entomopathogenic fungus Beauveria bassiana. PLoS Pathog. 2012/11/21
865 ed. 2012;8(11):e1003029.

866 71. Fraiture M, Baxter RHG, Steinert S, Chelliah Y, Frolet CC, Quispe-Tintaya W, et al. Two
867 Mosquito LRR Proteins Function as Complement Control Factors in the TEP1-Mediated
868 Killing of Plasmodium. Cell Host and Microbe. 2009/03/17 ed. 2009;5(3):273–84.

869 72. Ruiz VMR, Sousa GL, Sneed SD, Farrant KV, Christophides GK, Povelones M. Stimulation
870 of a protease targeting the LRIM1/APL1C complex reveals specificity in complement-like
871 pathway activation in Anopheles gambiae. PLOS ONE. 2019 Apr 8;14(4):e0214753.

872 73. Gupta S, Wang Y, Jiang H. Manduca sexta prophenoloxidase (proPO) activation requires
873 proPO-activating proteinase (PAP) and serine proteinase homologs (SPHs) simultaneously.
874 Insect Biochemistry and Molecular Biology. 2005 Mar;35(3):241–8.

875 74. Clark KD, Strand MR. Hemolymph melanization in the silkmoth Bombyx mori involves
876 formation of a high molecular mass complex that metabolizes tyrosine. J Biol Chem. 2013
877 May 17;288(20):14476–87.

878 75. Zhu Y, Wang Y, Gorman MJ, Jiang H, Kanost MR. Manduca sexta serpin-3 regulates
879 prophenoloxidase activation in response to infection by inhibiting prophenoloxidase-
880 activating proteinases. J Biol Chem. 2003 Nov 21;278(47):46556–64.

881 76. Christen JM, Hiromasa Y, An C, Kanost MR. Identification of plasma proteinase complexes
882 with serpin-3 in Manduca sexta. Insect Biochem Mol Biol. 2012 Dec;42(12):946–55.

883 77. Morejon B, Michel K. A zone-of-inhibition assay to screen for humoral antimicrobial activity
884 in mosquito hemolymph. Front Cell Infect Microbiol. 2023;13:891577.

885

886 **Tables**

887 **Table 1. List of proteins that co-immunoprecipitate with SRPN2**

AGAP number*	NCBI Acc. #	Gene Name	Molecular Weight (kDa)	Scaffold			Proteome Discoverer			
				Percent Coverage (%)	Unique Peptide Count	Total Spectrum Count	Score	Percent Coverage (%)	Total Peptide Count	# PSMs
AGAP006911	Q7QIJ8	SRPN2	47	52.8	13	26	99.29	53	13	28
AGAP008364	A0A453YTR1	TEP15	164	19.4	21	27	97.21	21	24	31
AGAP000376	Q7QF98	Transferrin	69	26.9	14	19	73.08	34	19	24
AGAP003250	C0L2J9	CLIPB4	39	33.1	8	11	45.76	36	9	14
AGAP006258	O44250	PPO1**	78	16.4	7	12	43.8	16	7	12
AGAP009217	Q7PVQ0	CLIPB12	38	22.3	5	6	32.9	34	8	11
AGAP004977	O96753	PPO6	79	14.1	6	9	30.87	16	7	10
AGAP011788	A0A1S4H7K2	CLIPA14	46	25.8	7	8	29.89	26	7	9
AGAP028138	Q5TPW1	Gelsolin	83	8.19	5	7	26.84	11	7	9
AGAP008060	Q6JEK4	Imaginal disc growth factor 2	48	8.66	3	3	16.12	16	6	6
AGAP003095	Q8MZM5	Dopachrome conversion enzyme	53	9.09	3	3	14.4	16	5	5
AGAP001377	Q005M5	SRPN11	57	14	5	5	13.85	14	5	5
AGAP003139	A0A1S4GHQ9	SRPN9	50	10.3	3	3	13.67	10	3	4
AGAP002564	F5HKV6	Fructose biphosphate aldolase	39	7.71	2	3	10.56	10	3	4
AGAP010968	A0A1S4H5E1	CLIPA9	40	7.18	2	3	9.22	7	2	3
AGAP011789	Q7PV63	CLIPA6	46	7.03	2	2	9.2	7	2	3
AGAP007406	Q7PT29	Elongation factor 1-alpha	50	7.56	2	2	8.92	11	3	3
AGAP010815	A0A2P1E488	TEP1	152	1.87	2	2	8.4	3	3	3
AGAP007037	F2Y0G4	APL1C	82	5.7	3	3	7.95	6	3	3
AGAP003689	A0A1S4GIW4	CLIPC7	67	4.19	2	2	5.82	4	2	2
AGAP010724	Q7PCX0	Histon H4	11	23.3	2	2	5.19	23	2	2
AGAP003691	A0A1S4GJE4	CLIPE12	98	3.13	2	2	4.88	3	2	2

*AGAP number based on AgamP4.13

888 **named PPO2 in VectorBase

889

890 **Figures**

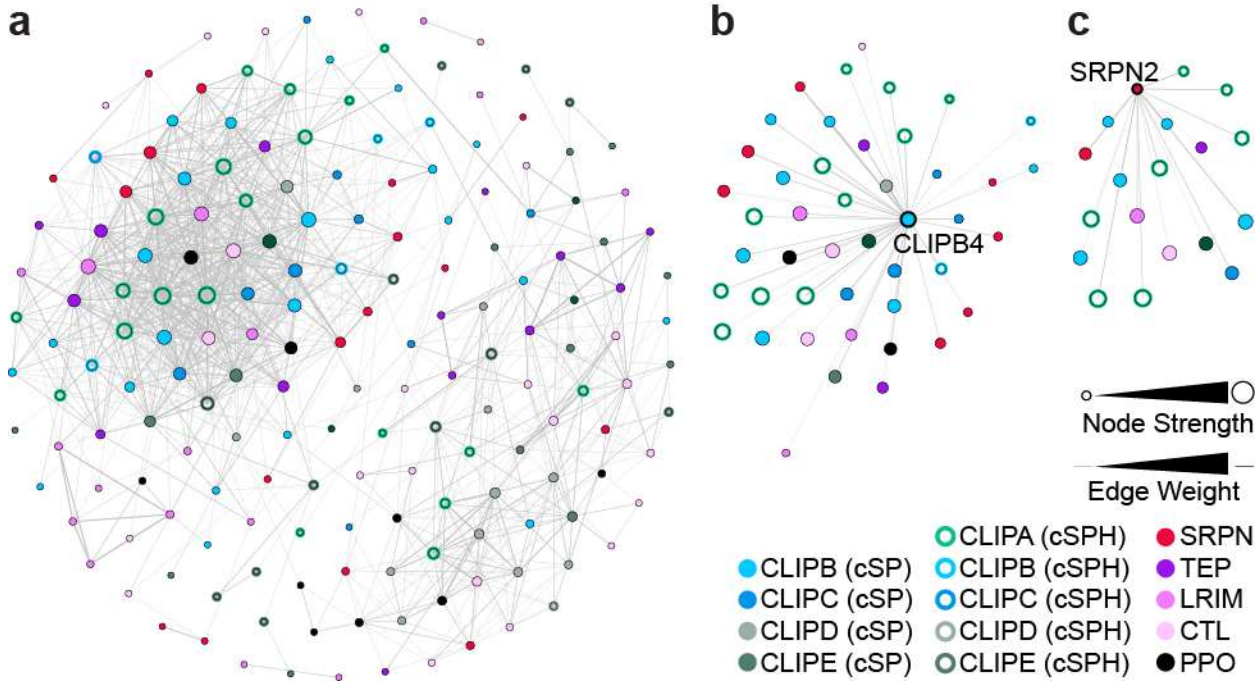

891

892 **Fig. 1. Gene co-expression network of genes with putative roles in melanization (AgMelGCN).**
893 (A) The network topography of AgMelGCN containing 178 nodes and 1229 edges. Of all
894 annotated putative CLIP serine proteases, CLIPB4 has the highest node degree in the network and
895 is co-expressed with SRPN2. (B) Genes in the network that are co-expressed with CLIPB4, which
896 includes SRPN2. (C) Genes in the network that are co-expressed with SRPN2, which includes
897 CLIPB4. The position of every node in the network visualization is identical in all three panels.

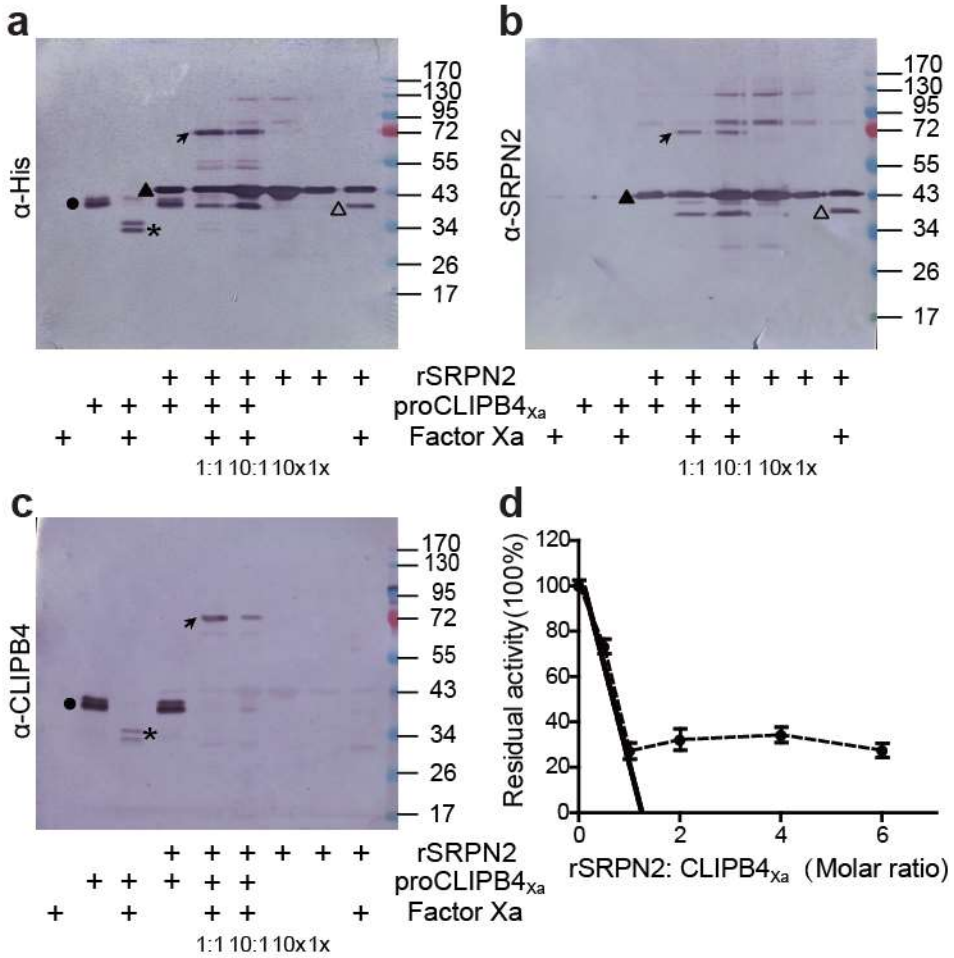

Fig. 2. SRPN2 forms SDS-stable complex with CLIPB4 and inhibits its activity. (**a**, **b**, **c**) Detection of CLIPB4-SRPN2 complex by immunoblot analysis. Recombinant proCLIPB4$_{Xa}$ was activated by Factor Xa, and then incubated with recombinant SRPN2 with a molar ratio of 1:1 or 10:1 (rSRPN2: proCLIPB4$_{Xa}$) at room temperature for 15 min. The mixtures were subjected to 12% SDS-PAGE followed by immunoblot analysis with mouse anti-His (**a**) or rabbit anti-SRPN2 (**b**) or rabbit anti-CLIPB4 (**c**) antibodies. Circles, the proCLIPB4$_{Xa}$ zymogen; asterisks, catalytic domain of proCLIPB4$_{Xa}$; solid triangles, recombinant SRPN2; hollow triangles, truncated SRPN2; *arrows*, CLIPB4/SRPN2 complex. (D) Stoichiometry of SRPN2 inhibition of CLIPB4. Factor Xa-activated CLIPB4 was incubated with recombinant SRPN2 at various molar ratios at room temperature for 15 min. Residual activities of CLIPB4 were measured with IEAR*p*NA as substrate and plotted as mean±1 SD (n=3) against the corresponding molar ratios of rSRPN2 and proCLIPB4$_{Xa}$.

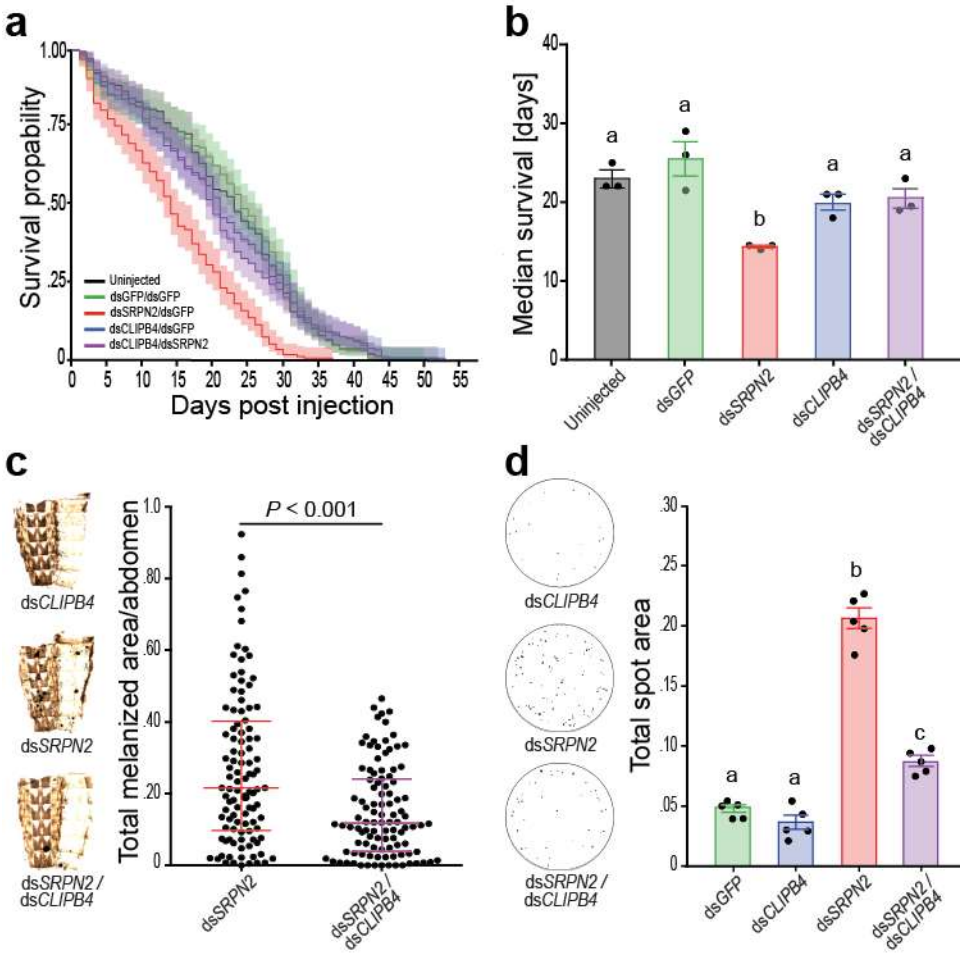

Fig. 3. ds*CLIPB4* partially recovers the phenotype of SRPN2 depletion. (**a**) *CLIPB4*kd alone did not affect survival rates, but reverted the increased mortality induced by SRPN2 depletion. Survival curves were plotted as means with 95% confidence intervals (n=3). (**b**) Median survivals in days were plotted (mean ± 1 SEM) based on results shown in (**a**); statistically significantly differences are indicated by different letters (one-way ANOVA followed by Newman-Keuls test, P<0.01). (**c**) Total melanotic area per abdomen decreased due to ds*CLIPB4* in SRPN2-depleted genetic background. Medians and interquartile ranges are marked (n=104, 5 biological replicates), and statistical analysis was performed with the Mann-Whitney U test. (**d**) SRPN2 depletion increased melanotic excreta, which was tempered partially by ds*CLIPB4* treatment. Data are shown as dots for individual replicates, bars represent means ± 1 SD (n = 5); Data were distributed normally (Shapiro-Wilk test, *P*<0.0001), and statistically significantly differences are indicated by different letters (one-way ANOVA followed by Newman-Keuls test, P<0.01).

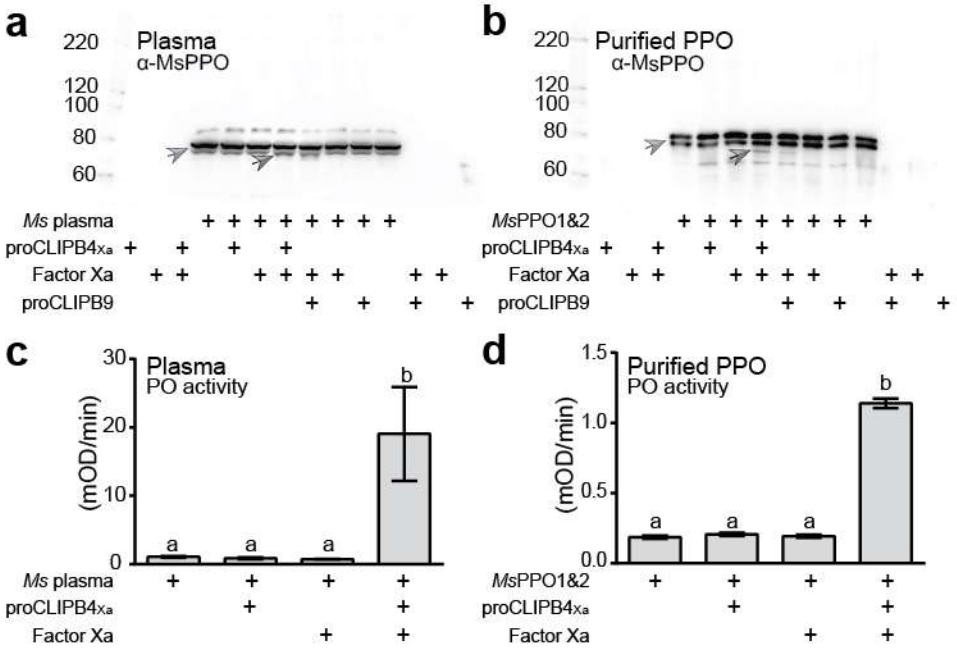

Fig. 4. CLIPB4 cleaves and activates *M. sexta* PPO1&2. Factor Xa-activated proCLIPB4$_{Xa}$ cleaves MsPPO1&2 in plasma (**a**) and purified protein (**b**), detected by immunoblot using rabbit anti-MsPPO1&2 antibody. The light and dark gray arrows indicate full and cleaved MsPPO1&2, respectively. CLIPB9 cleavage of *M. sexta* PPO was used as a positive control. The cleavage by CLIPB4 leads to increased PO activity in plasma (**c**) and with purified PPO protein (**d**). Bars represent mean ± 1 SD (n = 3); statistically significantly differences are indicated by different letters (one-way ANOVA followed by Newman-Keuls test, P<0.05).

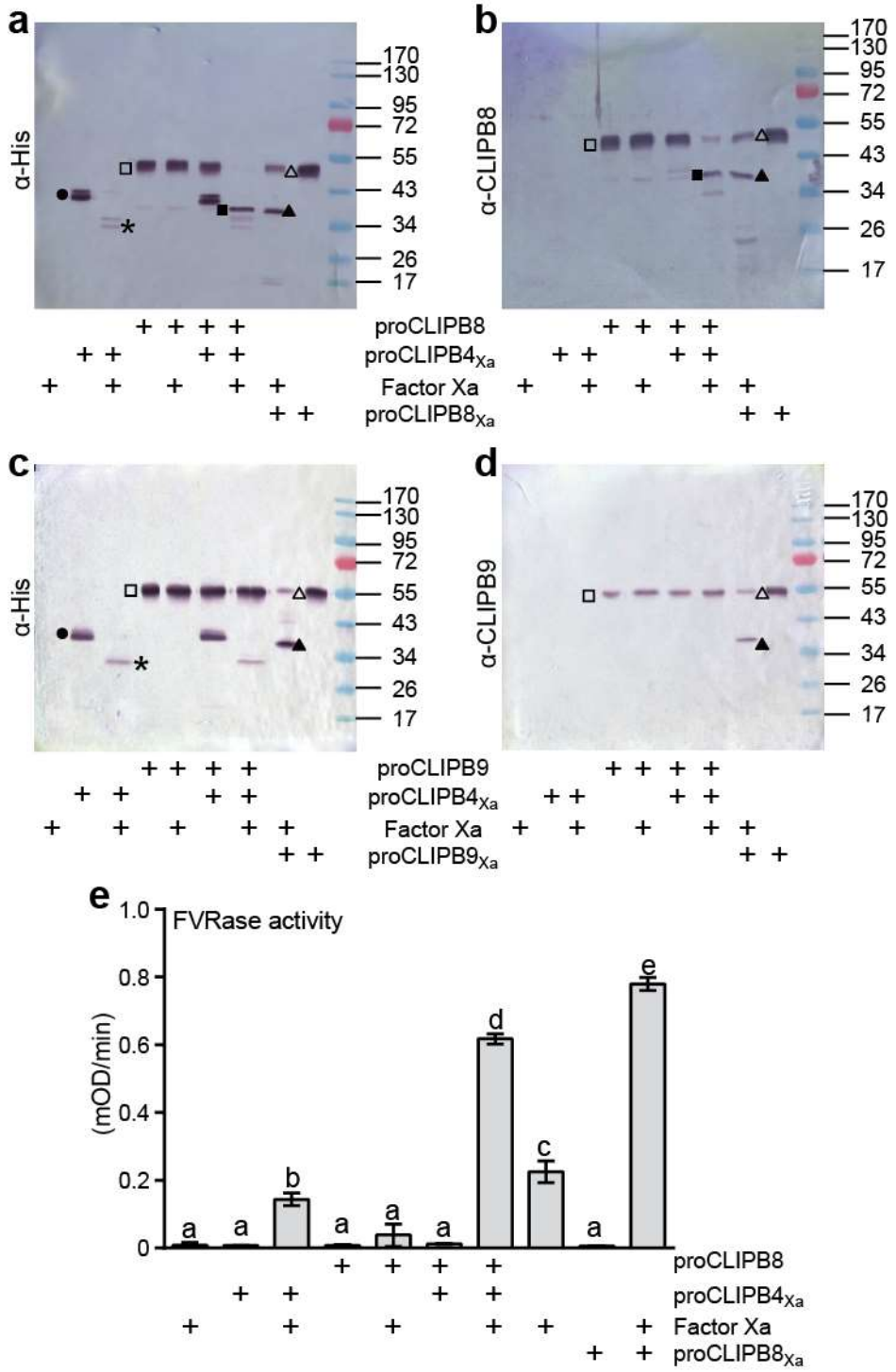

Fig. 5. CLIPB4 activates B8, not B9. Recombinant proCLIPB4$_{Xa}$ was activated by Factor Xa, and subsequently incubated with 100 ng of recombinant proCLIPB8 or proCLIPB9 at room temperature for 15 min. Samples were subjected to 12% SDS-PAGE followed by immunoblot with mouse anti-His (**a**, **c**), rabbit anti-CLIPB8 (**b**), and rabbit anti-CLIPB9 (**d**) antibodies,

937 respectively. In parallel, 100 ng of Factor Xa-activated proCLIPB8$_{Xa}$ or proCLIPB9$_{Xa}$ were used
938 as positive controls. Circles, proCLIPB4$_{Xa}$ zymogen; asterisks, catalytic domain of CLIPB4;
939 hollow squares, recombinant proCLIPB8 or proCLIPB9 zymogen; solid squares, catalytic domain
940 of proCLIPB8; hollow triangles, proCLIPB8$_{Xa}$ or proCLIPB9$_{Xa}$ zymogen; solid triangles, catalytic
941 domain of proCLIPB8$_{Xa}$ or proCLIPB9$_{Xa}$. (**e**) 72 ng of Factor Xa-activated proCLIPB4$_{Xa}$ was
942 incubated with 450 ng of recombinant proCLIPB8 at room temperature for 1 h, and the catalytic
943 activity of CLIPB8 was determined using FVR as substrate; 450 ng of Factor Xa-activated
944 proCLIPB8$_{Xa}$ was used as a positive control. ars represent mean ± 1 SD (n = 3); statistically
945 significantly differences are indicated by different letters (one-way ANOVA followed by
946 Newman-Keuls test, $P<0.05$).

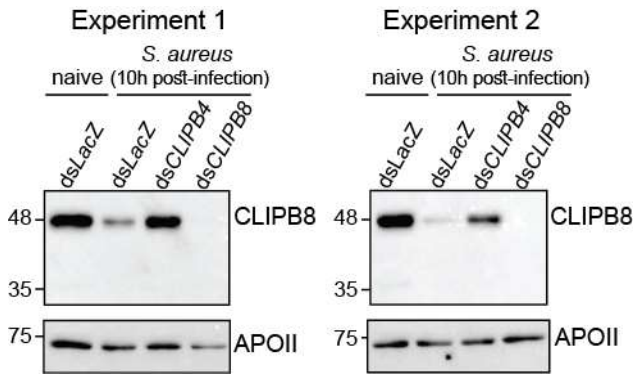

Fig. 6. CLIPB4 is required for infection-induced depletion of CLIPB8 from the hemolymph of *An. gambiae*. Female mosquitoes were treated by ds*LacZ*, ds*CLIPB4* and ds*CLIPB8*. Posted recovery, mosquitoes were challenged by *S. aureus* (OD_{600}=0.8). Ten hours post infection, hemolymph was collected by proboscis clipping, separated by SDS-PAGE, and subjected to immunoblot using rabbit anti-CLIPB8 and rabbit anti-APOII antibodies. Results were shown from two independent experiments.